

Figure 8a. Reproduced event m_b (PDE) as a function of event m_b (P), where reproduced PDE measurements are made using a time window length of 10 s (to approximate the time window used in the PDE bulletin). Measurements of m_b (P) are made using a 15 s time window and the distance and depth corrections for all magnitudes shown are Gutenberg-Richter (to match PDE bulletin). Correlation coefficient value (R) is shown for each of the six subsets of earthquakes (PDE bulletin m_b 5.0 to 5.5).

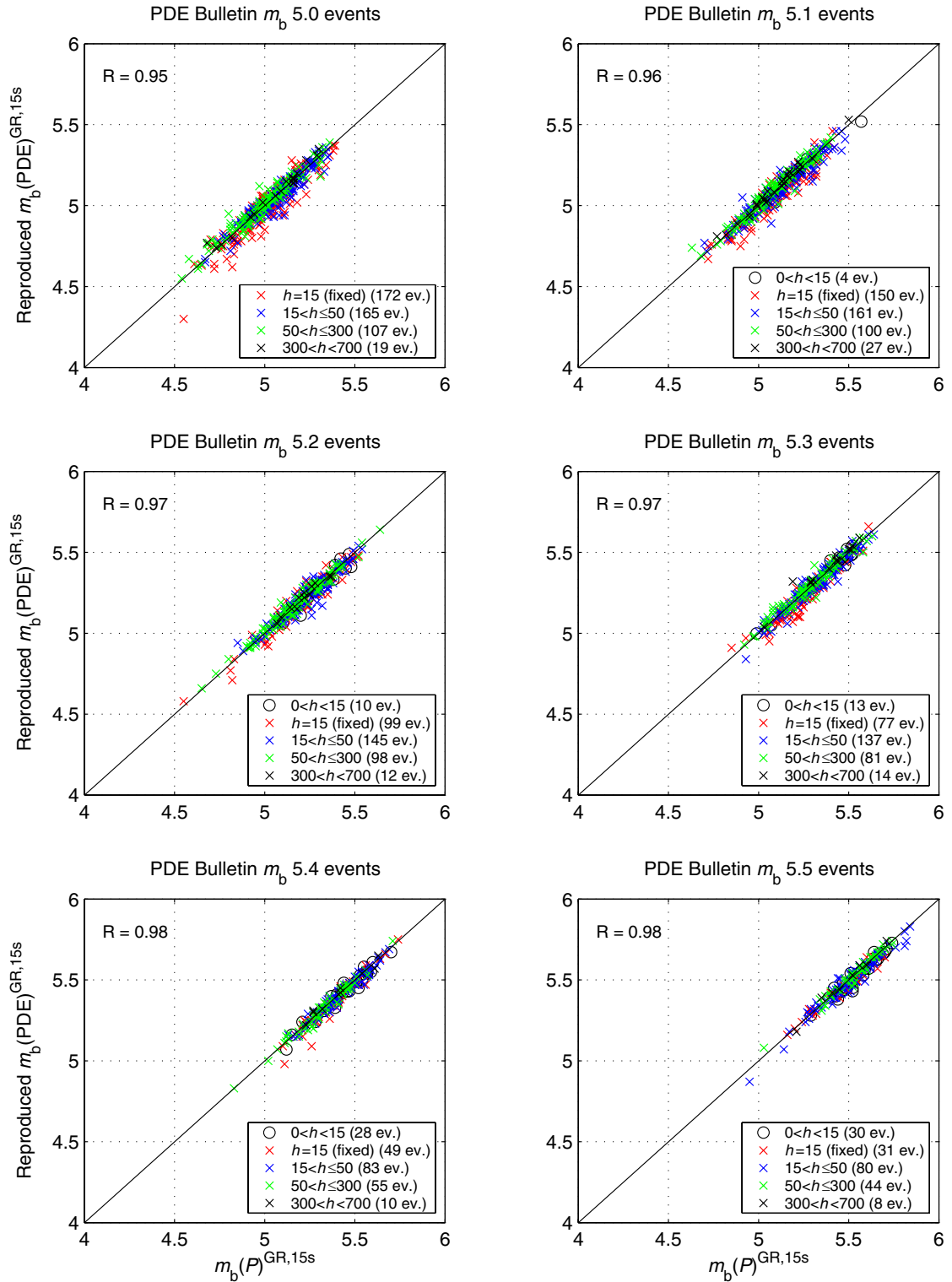


Figure 8b. Reproduced event $m_b(PDE)$ as a function of event $m_b(P)$, where both magnitude types are measured using a 15 s time window. Distance and depth corrections for all magnitudes shown are Gutenberg-Richter. Correlation coefficient value (R) is shown for each of the six subsets of earthquakes.

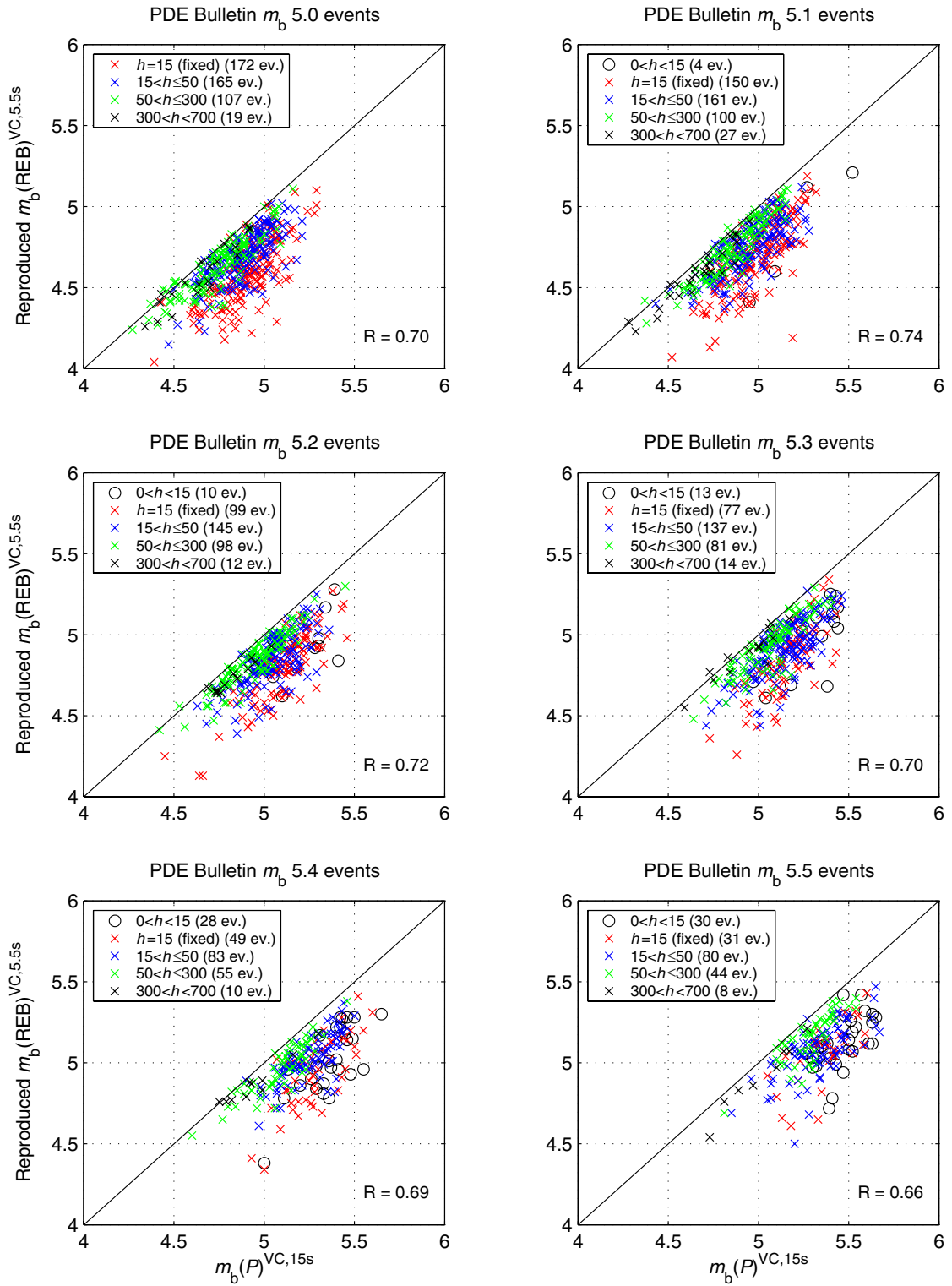


Figure 9a. Reproduced event $m_b(\text{ReB})$ as a function of event $m_b(P)$, where reproduced REB measurements are made using a time window length of 5.5 s (to match the time window used in the REB catalog). Measurements of $m_b(P)$ are made using a 15 s time window and the distance and depth corrections for all magnitudes shown are Veith-Clawson (to match REB catalog). Correlation coefficient value (R) is shown for each of the six subsets of earthquakes (PDE bulletin m_b 5.0 to 5.5).

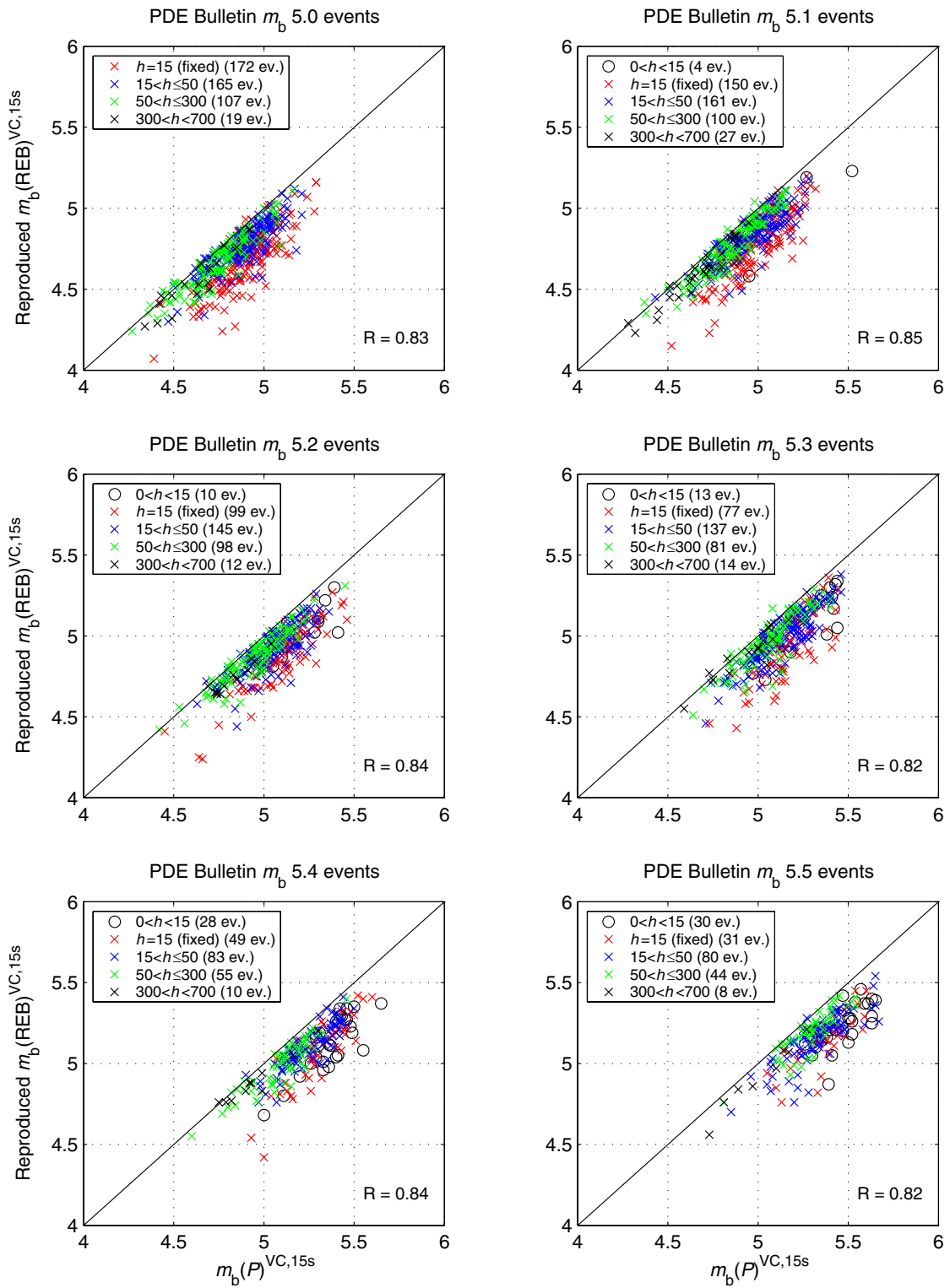


Figure 9b. Reproduced event $m_b(\text{ReB})$ as a function of event $m_b(P)$, where both magnitude types are measured using a 15 s time window. Distance and depth corrections for all magnitudes shown are Veith-Clawson. Correlation coefficient value (R) is shown for each of the six subsets of earthquakes.

Relationship between $m_b(P)$, M_w , and M_s

For this study, we selected earthquakes that have a Harvard CMT and moment magnitude (M_w) so that we can compare M_w to m_b . In Figure 1, we show the relationship between that M_w and $m_b(P)^{GR,15s}$ for each of the six subsets of data. We find little correlation between moment magnitude and body-wave magnitude, suggesting that seismic moment is only weakly related to the amplitude of short-period P -waves in this range of m_b . This result reinforces the fact that moment and body-wave magnitude are fundamentally different concepts – moment is a physically defined attribute whose value can be estimated from long-period data, whereas m_b is an empirically defined attribute whose value is directly measured according to a specific procedure (different for different scales).

Although we find little correlation between body-wave magnitude and moment magnitude, except that M_w is generally greater than m_b , previous studies using a much larger range of magnitudes have found a linear relationship between M_w and m_b (Rezapour, 2003; Sipkin, 2003), but with data scatter that exceeds one magnitude unit. The M_w - m_b results of these studies for m_b 5.0 to 5.5 earthquakes appear quite similar to the M_w - m_b relationship we find in Figure 1. Murphy and McLaughlin (1998) also studied the M_w - m_b relationship for a broader magnitude range of shallow ($h < 50$ km) earthquakes in the magnitude range $4.5 < m_b < 5.5$ and found that Harvard M_w estimates correlated quite well, on average, with conventional m_b and M_s measurements.

Although seismic moment provides the best estimate of earthquake size for many practical purposes, including tectonic interpretations and the analysis of fault mechanics, the moment magnitude derived from it should not be the only magnitude used for seismic

hazard studies. Moment magnitude is preferentially used for these types of studies because it better indicates the area over which strong shaking is likely to occur and is less affected than m_b by variations in Q ; however, m_b is more influenced than M_w by frequencies of interest to earthquake engineers. Thus, seismic hazard studies should include both m_b and M_w since m_b provides information about the source that M_w cannot, such as the strength of short-period ground shaking. Also, m_b , unlike M_w , is available for many events of $m_b < 5$. In contrast to the relationship between M_w and m_b , we find that the correlation between moment magnitude and surface-wave magnitude (M_s) is much stronger, with CMT M_w being greater than PDE bulletin M_s for nearly all events as shown in Figure 2. A stronger correlation between M_w and M_s is not surprising since both parameters are measured at long-periods whereas m_b is a short-period measurement.

References

- Murphy, J. R. and K. L. McLaughlin (1998). Comment on "Empirical determination of depth-distance corrections for m_b and M_w from Global Seismograph Network stations" by Guust Nolet, Steve Krueger, and Robert M. Clouser, *Geophys. Res. Lett.*, **25**, 4,269-4,270.
- Rezapour, M. (2003). Empirical global depth-distance correction terms for m_b determination based on seismic moment, *Bull. Seism. Soc. Am.*, **93**, 172-189.
- Sipkin, S. A. (2003). A correction to body-wave magnitude m_b based on moment magnitude M_w , *Seis. Res. Lett.*, **74**, 739-742.

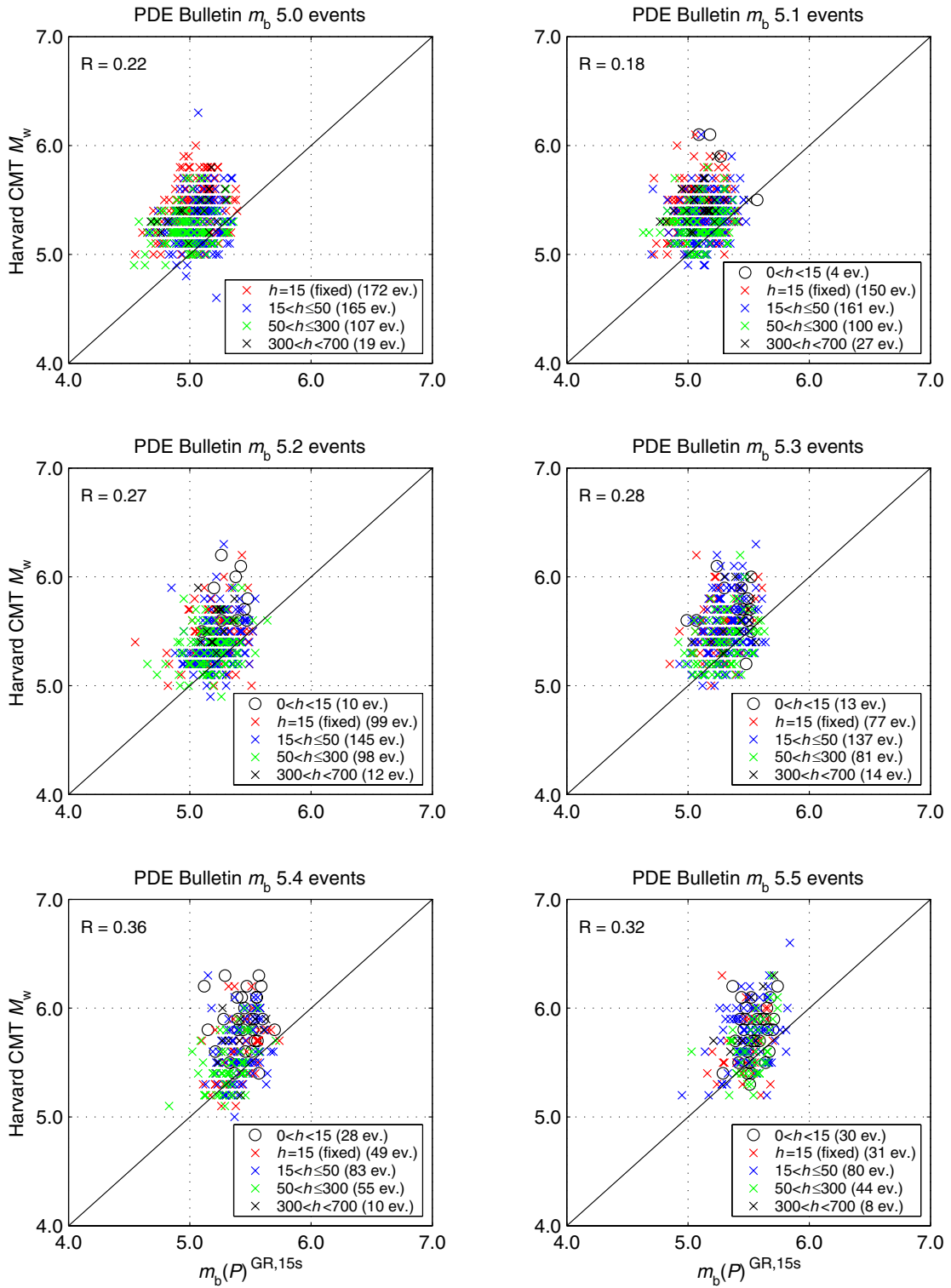


Figure 1. Harvard CMT event M_w as a function of event $m_b(P)$, for each of the six subsets of earthquakes (PDE bulletin m_b 5.0 to 5.5). Correlation coefficient (R) is shown for each plot.

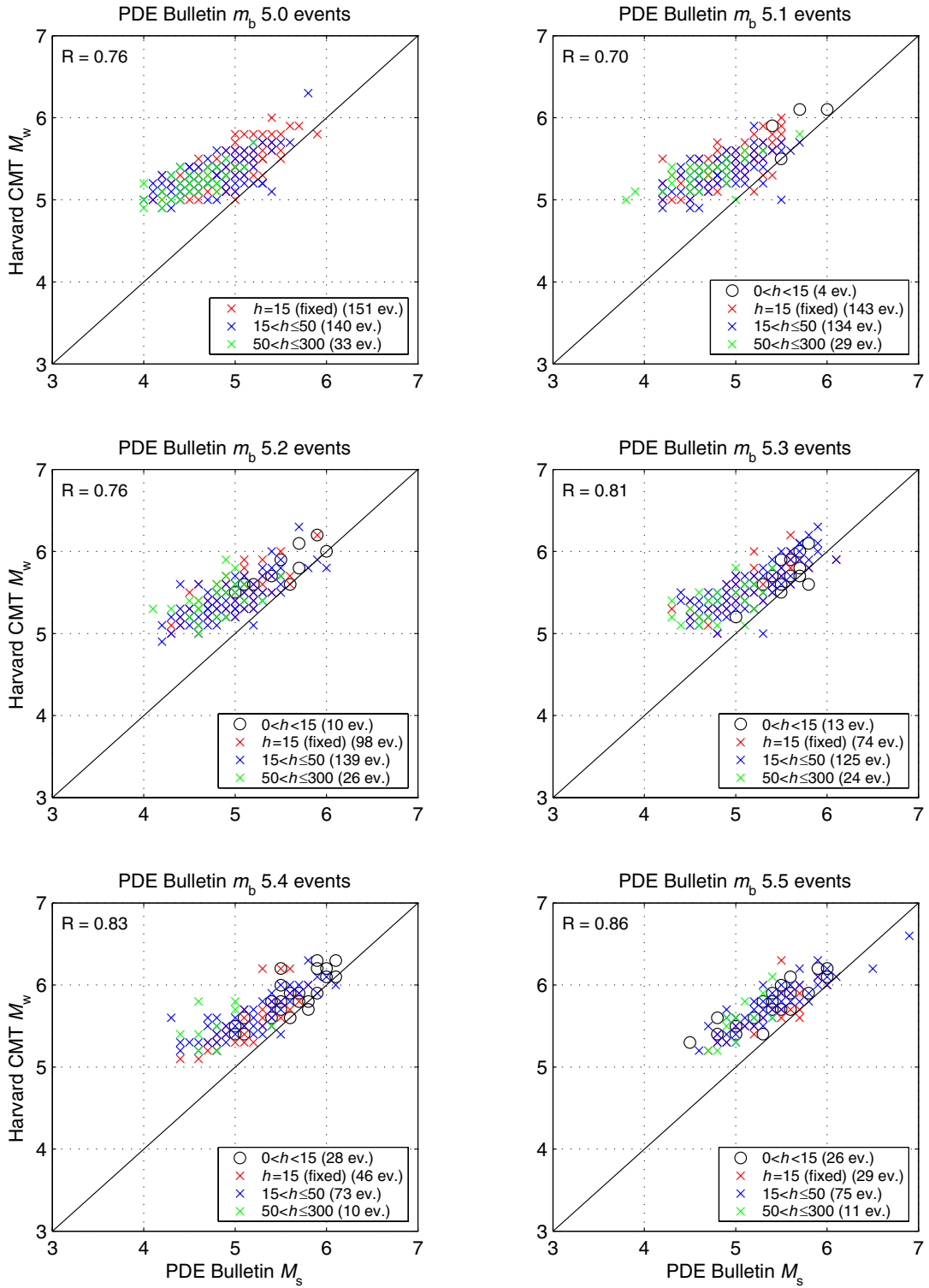


Figure 2. Harvard CMT event M_w as a function of PDE bulletin event M_s , for each of the six subsets of earthquakes (PDE bulletin m_b 5.0 to 5.5). Correlation coefficient (R) is shown for each plot.

Appendix 1

Parameterizing the Two USGS Filters as Poles and Zeros

To reproduce the measurements of signal amplitude and period published by the United States Geological Survey (USGS) in its Preliminary Determination of Epicenter (PDE) bulletin, we filter the broadband seismograms using a combination of two Butterworth bandpass filters. The filters are constructed according to an internal USGS memorandum (J. Dewey, personal communications since July 1998) and are applied to velocity signals. The first filter has a two pole highpass at 1.05 Hz and a two pole lowpass at 2.65 Hz; the second filter has a two pole highpass at 0.5 Hz and a two pole lowpass at 6.5 Hz. The combination of these two Butterworth filters produces a response function (in velocity) that has four zeros and eight poles. There are two poles corresponding to each of the four cutoff frequencies: 0.5 Hz, 1.05 Hz, 2.65 Hz, and 6.5 Hz.

The poles corresponding to each of the filter cutoff frequencies (ω_c) can be obtained from the transfer function for a second order Butterworth bandpass filter:

$$H(s) = (s^2 + \sqrt{2}s + 1)^{-1} \quad (\text{A1.1})$$

which has solutions (roots) at $s_1 = \omega_c[(-1/\sqrt{2}) + (i/\sqrt{2})]$ and $s_2 = \omega_c[(-1/\sqrt{2}) - (i/\sqrt{2})]$.

For the filter cutoff at 0.5 Hz, the cutoff frequency (ω_c) is given by:

$$\omega_c = 2\pi f = 2\pi(0.5) = \pi. \quad (\text{A1.2})$$

Thus, the two poles corresponding to this highpass cutoff are:

$$s_1 = \omega_c[(-1/\sqrt{2}) + (i/\sqrt{2})] = \pi[(-1/\sqrt{2}) + (i/\sqrt{2})] = -2.22144 + i(2.22144) \quad (\text{A1.3})$$

$$s_2 = \omega_c[(-1/\sqrt{2}) - (i/\sqrt{2})] = \pi[(-1/\sqrt{2}) - (i/\sqrt{2})] = -2.22144 - i(2.22144). \quad (\text{A1.4})$$

For the cutoff frequency of 1.05 Hz, ω_c is given by:

$$\omega_c = 2\pi(1.05) = 6.60. \quad (\text{A1.5})$$

The two poles corresponding to this highpass cutoff at 1.05 Hz are:

$$s_1 = (6.60)[(-1/\sqrt{2}) + (i/\sqrt{2})] = -4.66503 + i(4.66503) \quad (\text{A1.6})$$

$$s_2 = (6.60)[(-1/\sqrt{2}) - (i/\sqrt{2})] = -4.66503 - i(4.66503). \quad (\text{A1.7})$$

For the lowpass cutoff at 2.65 Hz, ω_c is given by:

$$\omega_c = 2\pi(2.65) = 16.7. \quad (\text{A1.8})$$

This lowpass cutoff at 2.65 Hz has poles at:

$$s_1 = (16.7)[(-1/\sqrt{2}) + (i/\sqrt{2})] = -11.7736 + i(11.7736) \quad (\text{A1.9})$$

$$s_2 = (16.7)[(-1/\sqrt{2}) - (i/\sqrt{2})] = -11.7736 - i(11.7736). \quad (\text{A1.10})$$

Finally, the lowpass cutoff at 6.5 Hz has an ω_c value of:

$$\omega_c = 2\pi(6.5) = 40.8. \quad (\text{A1.11})$$

This lowpass cutoff has solutions at:

$$s_1 = (40.8)[(-1/\sqrt{2}) + (i/\sqrt{2})] = -28.8787 + i(28.8787) \quad (\text{A1.12})$$

$$s_2 = (40.8)[(-1/\sqrt{2}) - (i/\sqrt{2})] = -28.8787 - i(28.8787). \quad (\text{A1.13})$$

Together, these eight pole values (equations A1.3-4, A1.6-7, A1.9-10, A1.12-13) completely describe the combination of the two Butterworth filters used by the USGS when assigning short-period magnitudes. This response function (described by four zeros and eight poles) is referred to as the USGS short-period velocity response. To obtain the equivalent displacement response, one zero must be added to the response function. This displacement response, based on the USGS filters, is shown in Figure 3.

Appendix 2

Parameterizing the PIDC Filter as Poles and Zeros

To duplicate the measurements published in the Reviewed Event Bulletin (REB) by the Prototype International Data Centre (PIDC), we filter the broadband seismograms using a third order, Butterworth bandpass filter. The PIDC filter is zero-phase, meaning that the filter is actually applied to the data twice – once in the forward direction and once in the reverse direction – to remove distortions in the waveform caused by a single pass of the filter. The filter is constructed based on the description given in *IDC Processing of Seismic, Hydroacoustic, and Infrasonic Data*¹ and is applied to velocity signals. This filter has a three pole highpass at 0.8 Hz and a three pole lowpass at 4.5 Hz, producing a response function (in velocity) that has six poles and three zeros.

The poles corresponding to each of the filter cutoff frequencies (ω_c) can be obtained from the transfer function for a third order Butterworth bandpass filter:

$$H(s) = [(s + 1)(s^2 + s + 1)]^{-1} \quad (\text{A2.1})$$

which has solutions (roots) at $s_1 = \omega_c[(-1) + i(0)]$, $s_2 = \omega_c[(-0.5) + i(\sqrt{3}/2)]$, and $s_3 = \omega_c[(-0.5) + i(-\sqrt{3}/2)]$.

For the filter cutoff at 0.8 Hz, the cutoff frequency (ω_c) is given by:

$$\omega_c = 2\pi f = 2\pi(0.8) = 5.03. \quad (\text{A2.2})$$

Thus, the three poles corresponding to this highpass cutoff are:

$$s_1 = \omega_c[(-1) + i(0)] = (5.03)[(-1) + i(0)] = -5.02655 + i(0) \quad (\text{A2.3})$$

$$s_2 = (5.03)[(-0.5) + i(\sqrt{3}/2)] = -2.51327 + i(4.35312) \quad (\text{A2.4})$$

$$s_3 = (5.03)[(-0.5) + i(-\sqrt{3}/2)] = -2.51327 - i(4.35312). \quad (\text{A2.5})$$

For the lowpass cutoff at 4.5 Hz, ω_c is given by:

$$\omega_c = 2\pi(4.5) = 28.3. \quad (\text{A2.6})$$

The three poles corresponding to this lowpass cutoff at 4.5 Hz are:

$$s_1 = \omega_c[(-1) + i(0)] = (28.3)[(-1) + i(0)] = -28.2743 + i(0) \quad (\text{A2.7})$$

$$s_2 = (28.3)[(-0.5) + i(\sqrt{3}/2)] = -14.1372 + i(24.4863) \quad (\text{A2.8})$$

$$s_3 = (28.3)[(-0.5) + i(-\sqrt{3}/2)] = -14.1372 - i(24.4863). \quad (\text{A2.9})$$

Since the PIDC uses a zero-phase Butterworth bandpass filter when assigning short-period magnitudes, the complete filter response consists of duplicate entries for each of the poles and zeros, reflecting the fact that the data are filtered twice using the same filter (once in the forward direction and once in the reverse direction). Thus, the complete response function (in velocity) consists of 12 poles and 6 zeros. To obtain the equivalent displacement response, a zero must be added to the velocity response function. The displacement response of the PIDC filter is shown in Figure 3.

¹ International Data Centre (1999). *IDC Processing of Seismic, Hydroacoustic, and Infrasonic Data*. Version 5.2.1, 233-255.